Journal of Materials Chemistry

Cite this: *J. Mater. Chem.*, 2011, **21**, 15629

www.rsc.org/materials

PAPER

Polymer based silver nanocomposites as versatile solid film and aqueous emulsion SERS substrates†

Sara Fateixa, Ana Violeta Girão, Helena I. S. Nogueira and Tito Trindade*

Received 31st May 2011, Accepted 1st August 2011
DOI: 10.1039/c1jm12444g

Nanocomposites containing Ag nanoparticles (average diameter ~11 nm) dispersed in poly(*tert*-butylacrylate) were prepared by *in situ* polymerization *via* miniemulsions and constitute active and versatile SERS substrates. The use of this synthetic strategy enables the dual use of the final composites as SERS substrates, both as aqueous emulsions and as cast films, shown here by several measurements using thiosalicylic acid as the testing analyte. The main advantage of these types of materials is related to the potential to scale up and the widespread use of handy substrates, using technology already available. This requires homogeneous composite substrates with SERS activity and this was demonstrated here by means of confocal Raman microscopy. Finally, a series of experiments were carried out on Ag/polymer nanocomposites submitted to temperature variations below and above the polymer glass transition temperature (T_g) in order to conclude about the effect of temperature processing conditions on the composites' SERS activity.

1. Introduction

Surface-Enhanced Raman scattering (SERS) is an optical detection method of Raman spectroscopy that gives structural and adsorption information on molecules attached to noble metal surfaces, typically of silver and gold.[1–6] This spectroscopic method involves localized vibrations of molecules chemisorbed at metal surfaces that exhibit a plasmonic response to the incident electromagnetic field. As a consequence, the shifts in the frequency of the scattered photons in relation to the incident monochromatic light appear as vibrational bands (Raman scattering) whose intensity can be enhanced up to a factor of 10^6 relative to conventional Raman spectroscopy.[7] This high sensitivity can reach down the molecular level[4] which, associated to recent technical and theoretical developments of SERS, opens up a number of perspectives of applications in analyte detection with particular interest in biosensing and environmental monitoring.[8–10]

In terms of materials for SERS substrates (in which the SERS effect may be observed for several analytes), and besides their chemical composition, the SERS effect observed for a specific analyte depends strongly on parameters related to a preferably nanostructured substrate, such as morphology and aggregation state.[5,6] This is because in specific nanoscopic junctions of the substrate, the local electromagnetic field can have an enhancement of several orders of magnitude due to local plasmonic coupling leading to the so-called "hot spots".[11–14] Therefore, the chemical design of new nanostructured substrates for SERS detection has been regarded as crucial to improve the use of this technique in diverse analytical conditions. The performance of such substrates can be optimized by creating "hot spots" that will depend, in the case of polymer composites, on the dispersion of the metal nanoparticles (NPs) within the polymer and on its retention capacity for the analyte.[14] Together with this electromagnetic model, there is also a chemical mechanism to consider in the interpretation of SERS.[5,6,15–17] The chemical contribution results from the charge transfer between the metal surface and the adsorbate molecule, and may help to explain the changes in the relative intensities of the Raman bands after adsorption in the metal surface. The wide implementation of SERS as an analytical tool requires that, associated to their high efficiency, the substrates should be fabricated in a reproducible and upscalable process, envisaging user-friendly characteristics.[18]

The implementation of polymer-based composites provides a plausible alternative to develop efficient and scalable supports for SERS. Braun *et al.* have reported a general strategy to nanoengineer hot spots in SERS substrates *via* nanoparticles linking, polymer coating and molecular permeation.[19] The polymer coating allows the retention of the analyte within the nanojunctions created by a set of Ag NPs wrapped by the polymer. However, this useful strategy requires a linking agent prior to the substrate preparation and has been reported for analyte detection in solution only. Examples of other polymer-based materials used for SERS include the incorporation of PVP/Ag colloidal solution on poly(methylmethacrylate) (PMMA) slides to provide durable SERS-active substrates,[20] the SERS analysis of Rhodamine 6G molecules adsorbed on a thin gold

Department of Chemistry and CICECO, University of Aveiro, 3810-193 Aveiro, Portugal. E-mail: tito@ua.pt; Fax: +351 234 370 084; Tel: +351 234 370 726

† Electronic supplementary information (ESI) available: Additional infrared and Raman spectra. See DOI: 10.1039/c1jm12444g

film deposited on polystyrene colloidal crystals,[21] SERS analysis of the PP vitamin onto a silver sol of PVP on a wide range of pH values[22] and solid Ag bionanocomposites of chitosan[23] and cellulose.[24]

In this work, we report for the first time the synthesis of polymer-based nanocomposites for SERS analysis using *in situ* miniemulsion polymerization in the presence of organically capped metal Ag nanoparticles. Poly(butyl)acrylate (PBA) was selected here as the polymer matrix based on our previous work with this polymer, that offers the possibility to incorporate metal NPs and originate surfaces that can be functionalized to produce beads sensitive to the surroundings.[25] In this way, versatile SERS substrates that can be used either as aqueous emulsions or as solid wafers could be produced. Moreover, the fabrication of these SERS substrates requires technology that is already available which in principle makes this strategy scalable in terms of synthesis and processing. In the present study we also examined the effect of temperature on the performance of the nanocomposites as SERS substrates. This is because polymer chain interactions, due to temperature variations above and below the glass transition temperature, can induce distinct states of aggregation for the metal NPs, hence variable interparticle distances that affect the SERS signal.

2. Experimental

The following chemicals were used as purchased: silver acetate ($Ag(CH_3CO_2)$, Sigma-Aldrich 99.9%); ethylene glycol (EG, Aldrich 99%); oleylamine (OA, Aldrich 70%); trioctylamine (TOA, Aldrich 98%); $NaHCO_3$ (Panreac 99%); potassium persulfate (KPS, Panreac 98%); dodecylsulfate sodium salt (SDS, Aldrich 98%); hexadecane (HD, Aldrich 99%). The monomers *tert*-butyl acrylate (*t*BA) and *n*-butyl acrylate (*n*BA) were purified over a column of neutral aluminium oxide and stored at 4 °C. Water was purified using a Sation 8000/Sation 9000 purification unit.

2.1. Synthesis of Ag-based nanocomposites

The organically capped silver nanoparticles were prepared using a modification of the polyol method described by Fievet *et al.*[26] as follows. A solution containing silver acetate (0.030 M) in ethylene glycol (10 mL) was injected into a hot solution containing 30 mL of trioctylamine and 10 mL of oleylamine (120 °C) for 30 min. The nanoparticles, after cooling at room temperature, were washed with 2-propanol and methanol (10 : 1) and isolated by centrifugation. This procedure was repeated twice to remove the excess of capping agent (TOA and OA). The nanoparticles were then dispersed in toluene. In order to obtain oleylamine capped silver nanoparticles, the $Ag(CH_3CO_2)$ was injected into OA at 120 °C for 30 minutes with or without ethylene glycol.

For the *in situ* polymerizations using miniemulsions, the procedure was as follows. For a 25 mL batch, the organically capped Ag NPs were homogeneously mixed with *t*BA or *n*BA (0.032 mol) and hexadecane (3.31×10^{-4} mol), to form a stable dispersion. This mixture was then mixed in an aqueous solution of dodecylsulfate sodium salt (SDS, 2×10^{-4} mol) and $NaHCO_3$ (9.81×10^{-4} mol) and was kept under vigorous stirring over 30 min, followed by sonication (amplitude 80%, 20 W power, Sonics-Vibracel Sonifier) for 7 min. The miniemulsion obtained was transferred to a conventional "*jacket*" glass reactor (30 mL capacity), equipped with a thermostatic bath, mechanical stirrer and nitrogen inlet. After purging with N_2, the temperature of the miniemulsion was set to 70 ± 1 °C and aqueous potassium persulfate (KPS, 6.78×10^{-5} mol) was added to the reaction, thus setting the zero time for the polymerization. The reaction took place over 4 h under mechanical stirring at 500 rpm. Monomer conversion was gravimetrically evaluated and typical values of 90% have been achieved.

2.2. SERS experiments

The Ag/P*t*BA nanocomposites were isolated and thoroughly washed with water using centrifugation steps. Solid nanocomposite substrates were obtained as cast films by simple evaporation from the aqueous emulsions. Solutions of thiosalicylic acid (TSA) with distinct concentrations (from 10^{-1} to 10^{-4} M) were prepared in ethanol to establish the lower detection limit for all the samples. A concentration of 10^{-3} M in TSA was generally used, although for some substrates the spectra could be obtained with a concentration of 10^{-4} M in the analyte. The samples for analysis were prepared by simple deposition of a drop of the analyte at the surface of the silver nanocomposite films or by injecting 20 μL of the analyte solution to 1 mL of the nanocomposite aqueous emulsion. The Raman spectra were recorded at several temperatures. For all SERS activity measurements, the pure polymer with deposited analyte was used as a control sample.

2.3. Instrumentation

The silver content in the nanocomposites was measured by Inductively Coupled Plasma Atomic Emission Spectroscopy (ICP-AES) using a Jobin-Yvon JY70Plus spectrophotometer. A Jasco V560 Ultra-Violet/Visible (UV/Vis) spectrophotometer was used for recording the UV/Vis absorption and reflectance spectra. The Fourier-transformed infrared spectra (FTIR) were recorded using a Matson 700 FTIR Spectrophotometer. Fourier-Transform (FT) Raman spectra were measured with 500 scans, using a Bruker RFS100/S FT-Raman spectrometer (Nd:YAG laser, 1064 nm excitation), at a power of 350 mV. The image in Fig. 6 was made with a WITec Raman imaging system using excitation from a Nd:YAG laser (532 nm) in a confocal Raman microscope. The SERS signal used for imaging was obtained by integrating over the 1012–1078 cm^{-1} region.

Transmission electron microscopy (TEM) was carried out on a Hitachi H-9000 TEM microscope operating at 300 kV or 200 kV. The TEM samples were prepared by placing a drop of the diluted colloid on a carbon-coated copper grid and the solvent was left to evaporate in air. Scanning electron microscopy (SEM) images were obtained using a Hitachi SU-70 SEM and EDX analysis was performed using an EDX Bruker Quantax 400.

Multimode tapping Atomic Force Microscopy (AFM) was carried out using a commercial multimode scanning probe microscope (Multimode, Nanoscope IIIA, DI). A commercial tip-cantilever normal silicon PPP-NCH-20 (Nanosensors) with

a spring constant of $k = 42$ N m^{-1} and typical tip radius of 7 nm, half-cone angle <10 at the last 200 nm of the tip, was used. Surface imaging was performed in the tapping mode, with resonance frequency at 190 kHz, at the scanning speed of 1–5 μm s^{-1}. The obtained images were evaluated using Scanning Probe Microscopy Software WSxM 4.0 free application, Nanotec Electronica S. L.[27]

3. Results and discussion

3.1. Synthesis and characterization of Ag/P*t*BA nanocomposites

Silver NPs have been prepared by reduction of $Ag(CH_3CO_2)$ in oleylamine and, in mixtures of oleylamine (OA) and trioctylamine (TOA) or ethylene glycol (EG). Table 1 indicates the reaction media and main characteristics of the Ag NPs prepared under these conditions (see FT-IR spectra in Fig. S1†).

The simple mixture of silver(I) acetate in oleylamine led to Ag NPs due to the reduction of cationic silver in the presence of imines derived from the thermal treatment of the solvent.[28] This synthesis produced a sample with the smallest average size and highest size dispersion, probably because in the absence of an additional reducing agent, silver(I) reduction is relatively slow which may allow the occurrence of secondary nucleations, thus resulting in a polydispersed sample. The addition of ethylene glycol to the reacting mixture led to a fast and more extensive Ag (I) reduction, forming metal nuclei in a shorter period of time followed by steady growth. As a consequence, the latter synthesis gave rise to Ag NPs with the lower size dispersion, in particular when a co-adjuvant organic capping ligand (TOA) has been added; this sample was selected for the nanocomposites preparation. Fig. 1 shows a typical TEM image for Ag NPs obtained in the latter conditions. X-Ray powder diffraction and electron diffraction patterns (not shown) confirmed the expected face-centred cubic (fcc) structure for metallic silver. The TEM image of the sample shows mainly round-shaped NPs (*ca.* 11 nm diameter) though particles having other shapes and bigger sizes have also been observed but in lesser amount.

In the past few years, miniemulsion polymerization has been reported as a powerful chemical method to produce aqueous emulsions of polymeric materials, including composites containing diverse types of inorganic NPs.[29–31] In previous works, we have shown that organically capped inorganic nanocrystals can

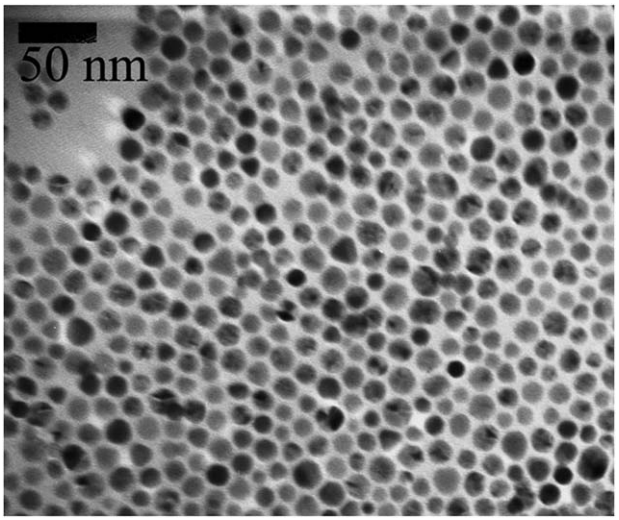

Fig. 1 TEM image of OA/TOA capped Ag NPs.

be employed as fillers to load polymers prepared *in situ*.[25,31,32] In brief, the chemical strategy requires the preparation of stable aqueous miniemulsions of monomer droplets into which organically capped nanoparticles can migrate. Initiation of polymerization of the monomer droplets results in aqueous emulsions of the metal/polymer nanocomposite and also in a certain amount of free polymer that can be removed by centrifugation. The final morphological characteristics of the nanocomposite particles depend, besides the polymerization conditions, on the ability of the monomer droplets to disperse the NPs in their interior. This in turn depends strongly on the NP size and on the nature of the organic capping at the particle surfaces. These results have been reproduced here for the first time for the encapsulation of Ag NPs in P*t*BA beads.

Fig. 2 shows the TEM image of a Ag/P*t*BA nanocomposite obtained after mini-emulsion polymerization in the presence of organically capped Ag NPs, in which the polymer contains the metal phase. The Ag/P*t*BA nanocomposite particle is formed by Ag nanoparticles clustered inside the polymer. In these composite particles, whose size varies around 150 to 300 nm, the Ag NPs were surrounded by a polymeric capsule with variable thickness. This was also confirmed by SEM and EDX that clearly show a thin polymeric capsule involving Ag NPs (Fig. 3). The P*t*BA capped Ag nanoparticles inside the capsule show a size

Table 1 Ag NP characteristics obtained in distinct reaction media, at 120 °C and under N_2

Reaction medium	SPR (λ_{max})/nm FWHM/nm[a]	Average diameter and size dispersion/nm[b]	IR diagnosis bands for the surface coat/cm^{-1}
$Ag(CH_3CO_2)$ Oleylamine	422 ± 0.2 84.6 ± 0.7	5.2 ± 3.2	3032 ν(=C–H); 2931, 2855 ν(–C–H); 1686 δ(N–H)
$Ag(CH_3CO_2)$ Oleylamine, ethylene glycol	413 ± 0.3 38.4 ± 0.9	7.3 ± 2.9	3006 ν(=C–H); 2914, 2847 ν(–C–H); 1745 δ(N–H)
$Ag(CH_3CO_2)$ Oleylamine Trioctylamine Ethylene glycol	418 ± 0.1 58.2 ± 0.2	11.2 ± 3.1	3006 ν(=C–H); 2914, 2855 ν(–C–H); 1745 δ(N–H); 1089 δ(=C–H)

[a] Surface plasmon resonance band maximum; full width at half maximum. [b] Measurements based on TEM.

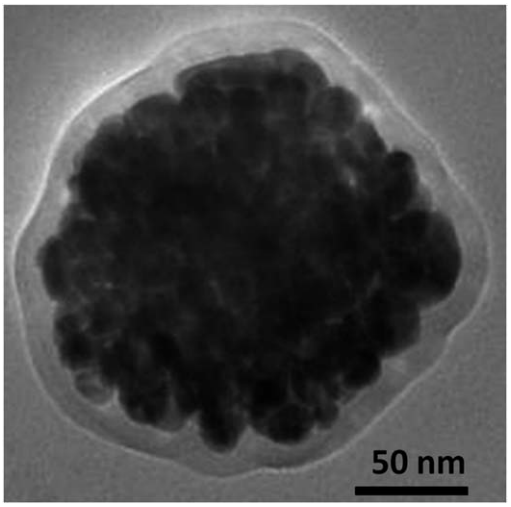

Fig. 2 TEM image of Ag/P*t*BA nanocomposite particle.

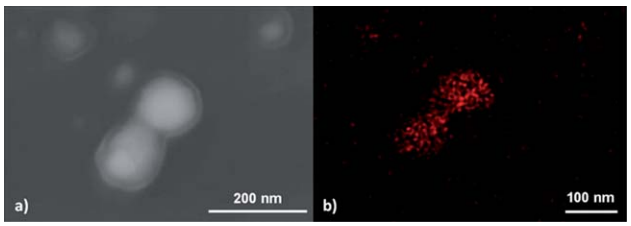

Fig. 3 SEM image (a) and EDX mapping (b) of silver NPs (red region) in Ag/P*t*BA nanocomposite beads.

distribution of 13.6 ± 3.9 nm, in accordance with the values of 11.2 ± 3.1 nm obtained for the Ag NPs alone (Table 1, last row) that are slightly smaller. Although this type of core/shell structure predominates in the composite sample, smaller and free particles have also been observed by TEM.

Similar to the gold nanocomposites reported previously,[25] effects on the surface plasmon resonance band of the Ag NPs are expected as a result of small changes in the dielectric surroundings and interparticle plasmon coupling. In fact, in Fig. 4 the SPR band is broader for the nanocomposite solid film and shows a bathochromic shift ($\Delta\lambda = 12$ nm) as compared to the optical spectrum of the starting Ag colloid. Note that the Ag NPs in the composite have a particle size distribution similar to those of the starting colloid.

3.2. SERS studies using Ag/PBA nanocomposites

Silver colloids and silver rough electrodes have been extensively used as SERS (Surface-Enhanced Raman Scattering) substrates to study diverse molecular analytes. This spectroscopic method allows enhancement factors up to 10^6 when compared to the conventional Raman signal, which makes SERS a powerful analytical tool to detect vestigial amounts of several compounds. Simultaneously, there has been an interest in developing new SERS substrates that make this type of analysis handy, versatile and faster. The nanocomposite materials described here have a new potential as SERS substrates because, in principle, they can be used in a dual form, either as aqueous emulsions or

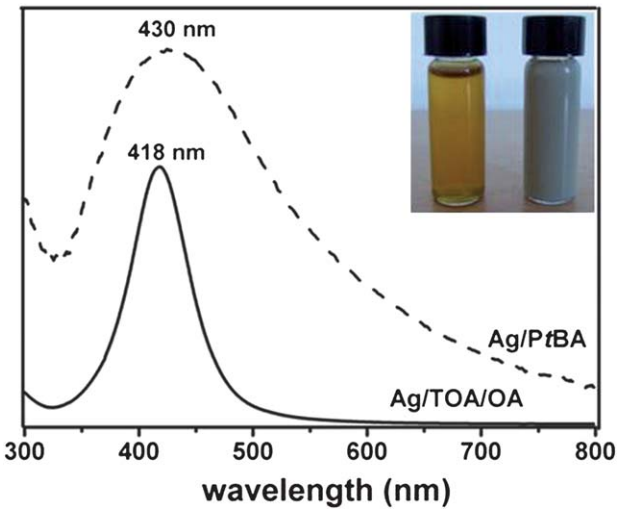

Fig. 4 UV/Visible spectra of organically capped Ag NPs in toluene and of a Ag/P*t*BA solid film (Kubelka–Munk units). The inset shows photographs of the Ag NPs in toluene (left) and of the Ag/P*t*BA aqueous emulsion (right).

mounted as solid wafers. This is of special interest in bioanalytical assays, in which the same type of analyte can be monitored in both states (either in colloidal suspensions or solid wafers) without changing the chemical nature of the substrate but the environmental conditions only.

The possibility to obtain SERS using the Ag/P*t*BA nanocomposites as substrates was investigated here in detail. Thiosalicylic acid (Fig. S2, ESI†) was used as the analyte probe in these SERS experiments, because this compound gives a good SERS signal in various analytical conditions.[24] Fig. 5 shows that the Raman spectrum of diluted thiosalicylic acid solution on the solid nanocomposite substrate is distinct from those of the nanocomposite Ag/P*t*BA alone and of the pure solid analyte (see shadow areas). The Raman spectra for the polymer P*t*BA alone and P*t*BA with a drop of thiosalicylic acid solution are very similar (Fig. S3, ESI†). Therefore, the vibrational features

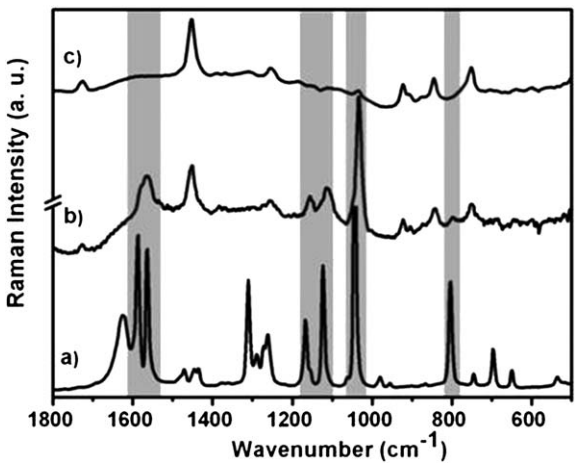

Fig. 5 (a) Conventional Raman spectrum for solid thiosalicylic acid; (b) SERS spectrum of a thiosalicylic acid aqueous solution (10^{-3} M) dropped in Ag/P*t*BA solid film; (c) Raman spectrum of a Ag/P*t*BA solid film.

observed in Fig. 5b can only be explained by the SERS effect due to the presence of Ag NPs in the polymer matrix.

The most striking changes in SERS in relation to the Raman spectrum of the solid compound (Fig. 5a) are the differences in the relative intensities of the most intense bands, and the simplification of the SERS spectrum where several bands are either not detected or show a very low intensity. When compared to the band at 1035 cm^{-1} assigned to δCH, there was a strong decrease in the intensity of the bands at 1559 and 1585 cm^{-1}, assigned to the νCC aromatic ring modes, and at 1630 cm^{-1} assigned to νC=O in the solid; a strong intensity decrease was also detected in the bands at 1151 (δCH, CH in-plane bending mode), 1119 (ν_{as}CX) and 798 cm^{-1} (νC–COOH). The band in the SERS spectrum at 1453 cm^{-1} assigned to P*t*BA hides the COO^- stretching mode ($\nu_s COO^-$) that would be expected around 1390 cm^{-1}. The adsorbed form is the thiosalicylate monoanion, as confirmed by the studies at varying pH shown below. Compared to SERS studies on 2-thionicotinic acid,[33] the thiosalicylate monoanion is thought to be adsorbed on the silver surface through the sulfur atom of the thiolate group and the adjacent oxygen atom of the carboxylate group, with the aromatic ring having a perpendicular position to the silver surface. The C–H stretching, νCH, is observed at 3053 cm^{-1}, supporting that the aromatic ring is perpendicular to the silver surface (Fig. S4, ESI†).

In this work, we have used confocal Raman microscopy to get evidence about the distribution of Ag NPs on the polymer cast films. Fig. 6 shows the Raman mapping in a solid sample of Ag/P*t*BA containing the analyte (thiosalicylic acid), based on the integrated intensity of the Raman signal in the 1012–1078 cm^{-1} region. This region corresponds to the SERS band assigned to aromatic δCH, the strongest in the SERS spectrum. Bright colours represent a more intense SERS signal and dark colours the weaker signals. The bright coloured areas correspond to regions of the nanocomposite in which the band integrated intensity increases. The intensity variation in this band is associated to the presence of Ag nanoparticles by assuming that this is a SERS signal due to the presence of thiosalicylic acid adsorbed at the silver surface. This constitutes an important tool to get a Raman mapping of the SERS active areas in the nanocomposite which in this particular case is quite homogeneous.

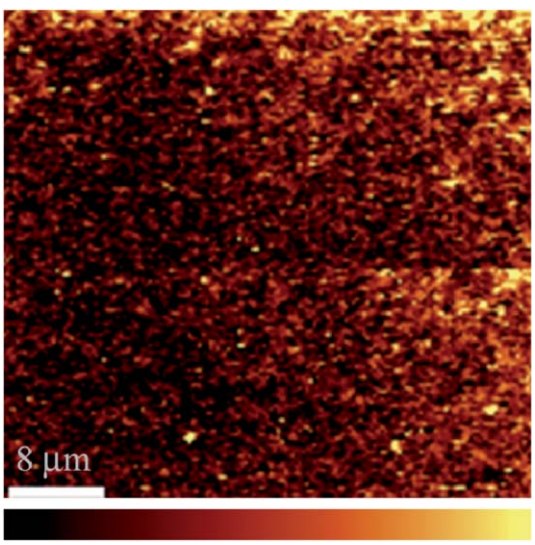

Fig. 6 Mapping of an Ag/P*t*BA composite film after addition of aqueous thiosalicylic acid, obtained by confocal Raman microscopy (integrated intensity of 1012–1078 cm^{-1} band). Bottom bar shows the colour profile, with signal integrated intensity increasing from left to right.

The dependence of SERS activity on analytical conditions such as the pH and the substrate temperature was evaluated. These experiments may help to clarify the interaction mode of the thiosalicylate molecules with the Ag NP surface, which is a requirement to observe SERS activity. Fig. 7 shows that the pH of the NP emulsion has a strong effect on the SERS signal of thiosalicylic acid when Ag/P*t*BA nanocomposites were used. Within the pH range used ($3 \leq pH \leq 10$), the polymer did not show significant changes (confirmed by IR spectroscopy) and the colloidal emulsions were stable for the period of SERS recording. Taking as reference the dissociation constants $pK_{a1} = 4.2$ (Ph–COOH) and $pK_{a2} = 9.3$ (Ph–SH) for the analyte (in water/ethanol 50%, at 25 °C)[34] the predominant species at neutral pH is the thiosalicylate monoanionic form, which in fact corresponds to the chemisorbed analyte at the silver surface as discussed above. The non-ionized form of thiosalicylate (pH = 3) and the dianionic sulfidobenzoate (pH = 10) seem less SERS active in the conditions of our experiments. Also, at high pH the composite is not chemically stable and probably the Ag NPs become less SERS active due to surface passivation.

It is generally accepted that SERS arises from a combination of an electromagnetic effect and a chemical contribution due to the interaction of the adsorbate at specific metal nanojunctions.[3,4] The electromagnetic effect depends on the excitation of localized surface plasmons by the incident light while the chemical effect results from charge transfer between the metal surface and adsorbate. It follows that the SERS spectra in Fig. 5 and 7 can only be understood in terms of a mechanism that promotes the chemisorption of thiosalicylate on Ag NPs. Although Fig. 3 shows Ag NPs coated with P*t*BA, which apparently could limit the chemisorption of thiosalicylate at the

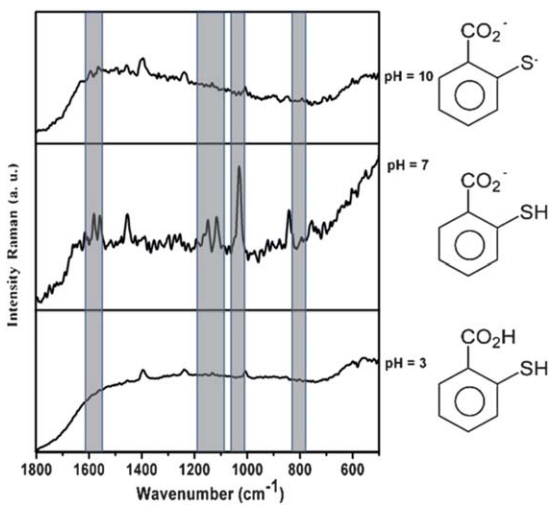

Fig. 7 SERS spectra of thiosalicylic acid using Ag/P*t*BA emulsions at variable pH.

silver surface, this is not necessarily the case because P*t*BA, as well as other (organic and inorganic) polymeric materials, forms porous coatings through which molecular species can diffuse.[35] In fact, this polymer seems to have beneficial consequences in terms of SERS efficiency because it may retain the analyte at the metal surfaces.

The incorporation of metal nanoparticles into a polymer matrix can bring about changes in the mechanical and thermal characteristics of the resulting composite. Moreover, the consequences of the processing conditions on the SERS activity need to be addressed.[36] In fact, this aspect is of great relevance when processing aims large scale and reproducible production of active SERS substrates. In the nanocomposites reported here, the mobility of the polymer chains may act as an additional pathway to alter the contact between the analyte and the metal surface when the nanocomposite is submitted to thermal treatment. To investigate this aspect, a series of SERS measurements have been performed at temperatures well below and above the glass transition temperature (T_g) of the nanocomposite that can be related to low and high mobility of the polymer chains, respectively.

The effect of the metal nanoparticles on the T_g of the polymer matrix has been reported for different nanoparticles and polymer composites, depending on several parameters whose influence is still an object of study.[37–40] The glass transition temperature of the nanocomposite was in this case determined by DSC measurements and, as shown in Fig. 8, it was observed at a slightly lower temperature (40 °C) than the T_g of the pure polymer (48 °C). These results suggest that the interaction of the polymer chains with the surface of the particles has an effect on the polymer interactions in the region immediately surrounding the particle due to the presence of the interface, making the chains more mobile.

Fig. 9 shows that the SERS spectra of thiosalicylic acid at 25 °C and 50 °C are very similar when using the Ag/P*t*BA nanocomposite. These results suggest that, at least in this temperature range, the changes occurring in the polymer do not have a marked effect on the formation of the metal–adsorbate complex. In order to have additional evidence for this type of behavior, we have performed a comparative experiment with a chemically similar polymer matrix but with a distinct T_g, by using the corresponding Ag nanocomposite of P*n*BA, which has

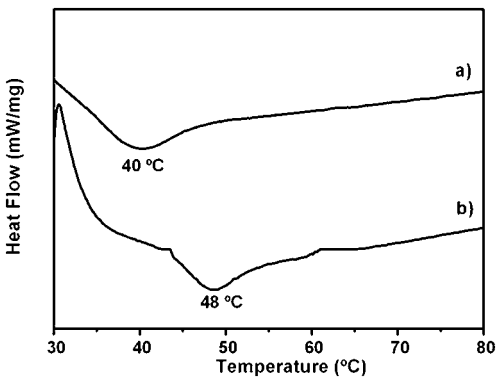

Fig. 8 DSC of (a) Ag/P*t*BA nanocomposites and (b) P*t*BA, both prepared by miniemulsion polymerization.

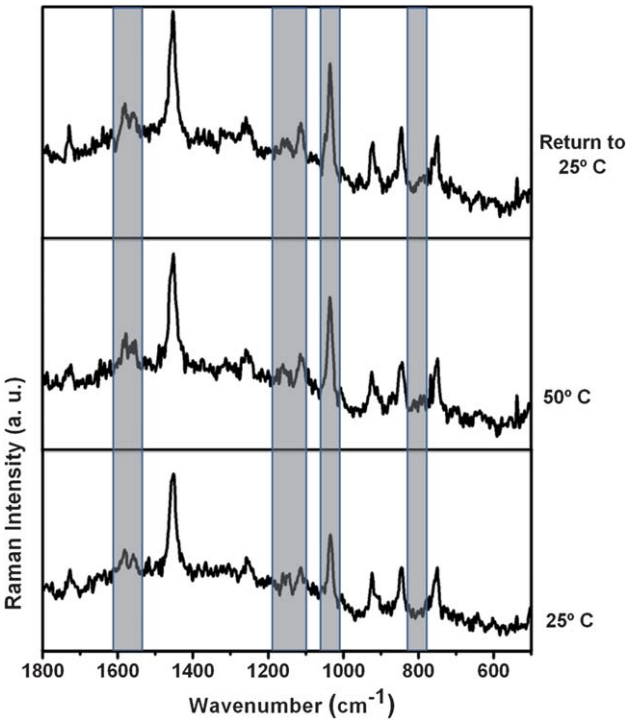

Fig. 9 SERS spectra of thiosalicylic acid in a Ag/P*t*BA film recorded at temperatures below and above the T_g (40 °C) of the nanocomposite.

a significantly lower T_g (−49 °C) as compared to P*t*BA. The SERS spectra for thiosalicylic acid in the Ag/P*n*BA nanocomposite were recorded (Fig. 10) in conditions similar to those performed for the Ag/P*t*BA material (Fig. S5, ESI†), by decreasing the temperature below the P*n*BA nanocomposite T_g (−49 °C). Although there is a slight decrease in the Raman intensity, which is most clear in the bands at 1570/1580 cm^{-1}, this is probably a temperature effect that has been reported in other situations[41,42] and is also observed here for the Ag/P*n*BA nanocomposite. Therefore, changes in the polymer chains' mobility due to temperature variation seem not to have a marked effect on the SERS signal of the analyte in the conditions investigated here. A possible explanation relies on the fact that the most determining factor for these types of nanocomposites to become SERS active relates to the availability of Ag surfaces that allows the chemisorption of the analyte. As a consequence, the molecules of thiosalicylic acid are still adsorbed at the Ag surfaces within the temperature range used in our experiments.

Finally, an important issue remains related to the performance of the Ag/P*t*BA nanocomposites as SERS substrates when submitted to a variable temperature before sample preparation. Indeed, the fact that changes in the mobility of the chains do not significantly affect the adsorbate complex once it is formed does not mean that the characteristics of the nanocomposite substrate have no effect on the SERS analysis prior to the preparation of samples. In this sense, the following experiments were performed to elucidate this aspect. The nanocomposites of Ag/P*t*BA were subjected to variations in temperature before the deposition of an aliquot of the thiosalicylic acid solution, and subsequently used as SERS substrates (Fig. 11) at room temperature. Clearly, the SERS signal appears attenuated in these situations as compared

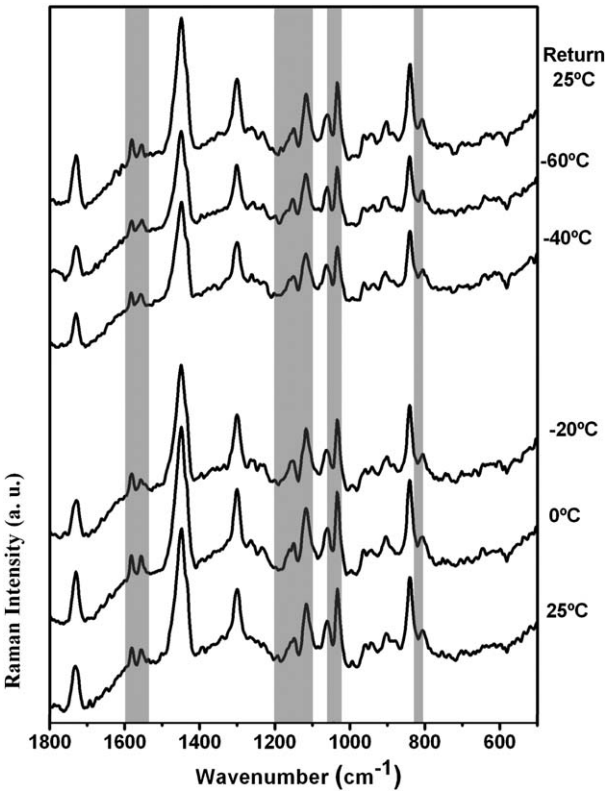

Fig. 10 SERS spectra for thiosalicylic acid in a Ag/P*n*BA film recorded at variable temperatures.

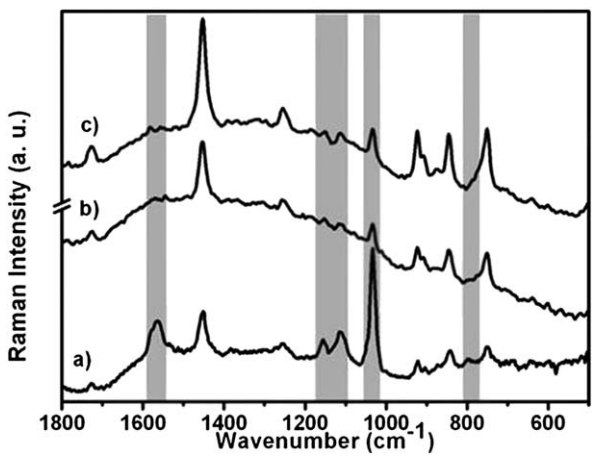

Fig. 11 SERS spectrum of thiosalicylic acid solution dropped in (a) Ag/P*t*BA solid film at 25 °C, (b) Ag/P*t*BA solid film after heating at 65 °C and (c) Ag/P*t*BA solid film after immersion in liquid nitrogen.

to the non-treated substrate, which suggests that the chemisorption of the analyte onto the Ag surfaces is a less favorable process. One possible explanation is that the re-organization of the polymer chains following the temperature variation led to a less number of hot spots in the nanocomposite. This could be possible by several mechanisms that, associated to a less favorable texture to chemisorption, hamper the diffusion of thiosalicylic acid molecules towards Ag active sites. AFM analysis performed on these treated substrates shows an increase in the surface roughness of the nanocomposite (Fig. 12), which possibly

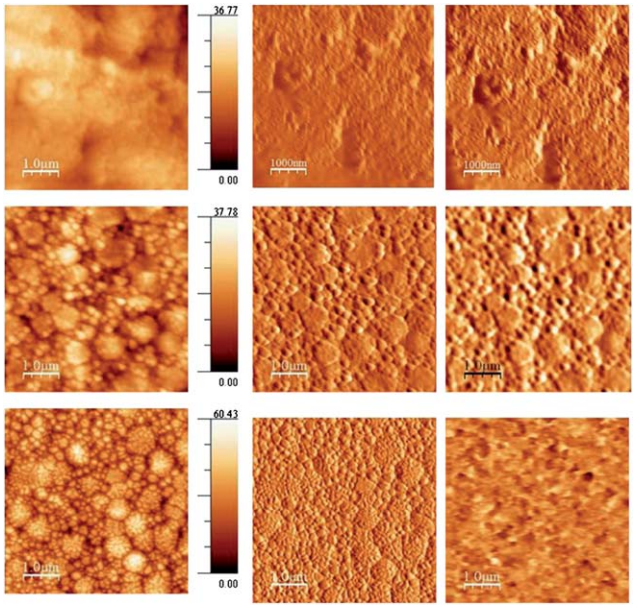

Fig. 12 AFM images (height—left side; amplitude—centre; phase—right side) obtained for a Ag/P*t*BA nanocomposite cast film at: 25 °C (upper panel, average roughness = 2.30); after 1 h at 65 °C (middle panel, average roughness = 3.56); after being immersed in liquid nitrogen (lower panel, average roughness = 6.86).

gives rise to an increase in the surface area that is not active in SERS, and that competes with Ag for the thiosalicylic acid sorption. It is noted that this increase in roughness is not necessarily an enhancement factor of the SERS signal, unlike what happens in pure silver electrodes, since in this case we have a composite in which the main component is the polymer, *i.e.* a SERS non-active surface.

4. Conclusions

Polymer (P*t*BA) based nanocomposites incorporating silver NPs have been prepared *via* polymerization in miniemulsions. This work demonstrated the potential of this approach not only to produce nanocomposite materials that are SERS active but also that contributes to implement SERS as an analytical tool in a wider context, such as the availability of scalable, versatile and handy substrates. Furthermore, the Ag/P*t*BA materials showed SERS activity when submitted to drastic temperature variations, at least within the temperature range investigated here (−60 °C to 65 °C), which suggest that the adsorbates are retained at the Ag sites eventually protected by the polymer layers. These materials might enable the development of new devices useful for clinical diagnosis eventually by promoting the biofunctionalization of the polymer matrix, which for the case of P*t*BA is easily accessed by hydrolytic and activation reactions.

Acknowledgements

We thank Fundacão para a Ciência e Tecnologia (FCT/FEDER) for the following grants: SFRH/BD/66460/2009 (S. Fateixa); SFRH/BPD/66407/2009 (A. Girão); project PTDC/QUI/67712/2006. Microscopy analysis was supported by RNME-Pole UA

FCT Project REDE/1509/RME/2005. The authors thank the assistance of Dr Nuno Mendes (UA) for the Raman analysis as a function of temperature and of Dr Ute Schmidt (WITec) for the confocal Raman microscopy.

Notes and references

1 D. L. Jeanmaire and R. P. Van Duyne, *J. Electroanal. Chem.*, 1977, **84**, 1.
2 M. G. Albrecht and J. A. Creighton, *J. Am. Chem. Soc.*, 1977, **99**, 5215.
3 M. Moskovits, *J. Chem. Phys.*, 1978, **69**, 4159.
4 K. Kneipp, H. Kneipp, I. Itzkan, R. R. Dasari and M. S. Feld, *Chem. Rev.*, 1999, **99**, 2957.
5 H. I. S. Nogueira, J. J. C. Teixeira-Dias and T. Trindade, *Nanostructured Metals in Surface Enhanced Raman Spectroscopy, Encyclopedia of Nanoscience and Nanotechnology*, ed. H. S. Nalwa, ASP, 2004, vol. 7, p. 699.
6 R. Aroca, *Surface-Enhanced Vibrational Spectroscopy*, John Wiley & Sons, 2006.
7 J. Comyn, J. A. Creighton, D. Landolt, H. J. Mathieu and R. Schumacher, *Anal. Proc.*, 1993, **30**, 27.
8 R. A. Tripp, R. A. Dluhy and Y. Zhao, *Nano Today*, 2008, **3**, 31.
9 J. Qian, L. Jiang, F. Cai, D. Wang and S. He, *Biomaterials*, 2011, **32**, 1601.
10 R. A. Halvorson and P. J. Vikesland, *Environ. Sci. Technol.*, 2010, **44**, 7749.
11 J. P. Camden, J. A. Dieringer, Y. Wang, D. J. Masiello, L. D. Marks, G. C. Schatz and R. P. Van Duyne, *J. Am. Chem. Soc.*, 2008, **130**, 12616.
12 P. H. C. Camargo, C. M. Cobley, M. Rycenga and Y. Xia, *Nanotechnology*, 2009, **20**, 434020.
13 S. M. Stranahan and K. A. Willets, *Nano Lett.*, 2010, **10**, 3777.
14 S. Abalde-Cela, S. Ho, B. Rodriguez-Gonzalez, M. A. Correa-Duarte, R. A. Alvarez-Puebla, L. M. Liz-Marzan and N. A. Kotov, *Angew. Chem., Int. Ed.*, 2009, **48**, 5326.
15 Y. Wu, J.-F. Li, B. Ren and Z.-Q. Tian, *Chem. Soc. Rev.*, 2008, **37**, 1025.
16 M. Fana, G. F. S. Andrade and A. G. Brolo, *Anal. Chim. Acta*, 2011, **693**, 7.
17 S. E. J. Bell and N. M. S. Sirimuthu, *Chem. Soc. Rev.*, 2008, **37**, 1012.
18 X. Liu, C.-H. Sun, N. C. Linn, B. Jiang and P. Jiang, *J. Phys. Chem. C*, 2009, **113**, 14804.
19 G. B. Braun, S. J. Lee, T. Laurence, N. Fera, L. Fabris, G. C. Bazan, M. Moskovits and N. O. Reich, *J. Phys. Chem. C*, 2009, **113**, 13622.
20 W. Lin, *Appl. Phys. A: Mater. Sci. Process.*, 2011, **102**, 121.
21 L. Lu, I. Randjelovic, R. Capek, N. Gaponik, J. Yang, H. Zhang and A. Eychmüller, *Chem. Mater.*, 2005, **17**, 5731.
22 T. Iliescu, S. Cinta, S. Astilean and I. Bratu, *J. Mol. Struct.*, 1997, **410–411**, 193.
23 M. Potara, A.-M. Gabudean and S. Astilean, *J. Mater. Chem.*, 2011, **21**, 3625.
24 P. A. A. P. Marques, H. I. S. Nogueira, R. J. B. Pinto, C. P. Neto and T. Trindade, *J. Raman Spectrosc.*, 2008, **39**, 439.
25 M. A. Martins, S. Fateixa, A. V. Girão, S. S. Pereira and T. Trindade, *Langmuir*, 2010, **26**, 11407.
26 F. Fievet, J. P. Lagier, B. Blin, B. Beaudoin and M. Figlarz, *Solid State Ionics*, 1989, **32–33**, 198.
27 I. Horcas, R. Fernández, J. M. Gómez-Rodríguez, J. Colchero, J. Gómez-Herrero and A. M. Baro, *Rev. Sci. Instrum.*, 2001, **78**, 013705.
28 M. Chen, Y.-G. Feng, X. Wang, T.-C. Li, J.-Y. Zhang and D.-J. Qian, *Langmuir*, 2007, **23**, 5296.
29 E. Bourgeat-Lami and M. Lansalot, *Adv. Polym. Sci.*, 2011, **233**, 53.
30 K. Landfester, *Angew. Chem., Int. Ed.*, 2009, **48**, 4488.
31 A. S. Pereira, P. Rauwel, M. S. Reis, N. J. Silva, A. M. Barros-Timmons and T. Trindade, *J. Mater. Chem.*, 2008, **18**, 4572.
32 A. C. C. Esteves, A. M. Barros-Timmons, T. Monteiro and T. Trindade, *J. Nanosci. Nanotechnol.*, 2005, **5**, 766.
33 H. I. S. Nogueira, *Spectrochim. Acta, Part A*, 1998, **54**, 1461.
34 K. A. Idriss, M. S. Saleh, M. M. Seleim and E. Y. Hashem, *J. Solution Chem.*, 1993, **22**, 469.
35 R. A. Álvarez-Puebla, R. Contreras-Cáceres, I. Pastoriza-Santos, J. Pérez-Juste and L. M. Liz-Marzán, *Angew. Chem., Int. Ed.*, 2009, **48**, 138.
36 M. Geissler, K. Li, B. Cui, L. Clime and T. Veres, *J. Phys. Chem. C*, 2009, **113**, 17296.
37 B. J. Ash, L. S. Schadler and R. W. Siegel, *Mater. Lett.*, 2002, **55**, 83.
38 V. V. Vodnik, D. K. Božanić, E. Džunuzović, J. Vuković and J. M. Nedeljković, *Eur. Polym. J.*, 2010, **46**, 137.
39 Y. M. Cao, J. Sun and D. H. Yu, *J. Appl. Polym. Sci.*, 2002, **83**, 70.
40 J. Q. Pham, C. A. Mitchell, J. L. Bahr, J. M. Tour, R. Krishanamoorti and P. F. Green, *J. Polym. Sci., Part B: Polym. Phys.*, 2003, **41**, 3339.
41 K.-H. Yang, Y.-C. Liu and T.-C. Hsu, *J. Electroanal. Chem.*, 2009, **632**, 184.
42 H.-P. Chiang, P. T. Leung and W. S. Tse, *J. Phys. Chem. B*, 2000, **104**, 2348.

